

Article

On Monotonic Pattern in Periodic Boundary Solutions of Cylindrical and Spherical Kortweg–De Vries–Burgers Equations

Alexey Samokhin

Trapeznikov Institute of Control Sciences, Russian Academy of Sciences, 65 Profsoyuznaya Street, 117997 Moscow, Russia; a.samohin@mstuca.aero or samohinalexey@gmail.com

Abstract: We studied, for the Kortweg–de Vries–Burgers equations on cylindrical and spherical waves, the development of a regular profile starting from an equilibrium under a periodic perturbation at the boundary. The regular profile at the vicinity of perturbation looks like a periodical chain of shock fronts with decreasing amplitudes. Further on, shock fronts become decaying smooth quasi-periodic oscillations. After the oscillations cease, the wave develops as a monotonic convex wave, terminated by a head shock of a constant height and equal velocity. This velocity depends on integral characteristics of a boundary condition and on spatial dimensions. In this paper the explicit asymptotic formulas for the monotonic part, the head shock and a median of the oscillating part are found.

Keywords: Korteweg–de Vries–Burgers equation; cylindrical and spherical waves; saw-tooth solutions; periodic boundary conditions; head shock wave

MSC: 35Q53; 35B36



Citation: Samokhin, A. On Monotonic Pattern in Periodic Boundary Solutions of Cylindrical and Spherical Kortweg–De Vries–Burgers Equations. *Symmetry* **2021**, *13*, 220. <https://doi.org/10.3390/sym13020220>

Academic Editors: Jan Awrejcewicz and Valentin Lychagin
Received: 22 December 2020
Accepted: 26 January 2021
Published: 29 January 2021

Publisher’s Note: MDPI stays neutral with regard to jurisdictional claims in published maps and institutional affiliations.



Copyright: © 2021 by the author. Licensee MDPI, Basel, Switzerland. This article is an open access article distributed under the terms and conditions of the Creative Commons Attribution (CC BY) license (<https://creativecommons.org/licenses/by/4.0/>).

1. Introduction

The well known Korteweg–de Vries (KdV)–Burgers equation for flat waves is of the form

$$u_t = -2uu_x + \varepsilon^2 u_{xx} + \delta u_{xxx}. \quad (1)$$

Its cylindrical and spherical analogues are

$$u_t + \frac{1}{2t}u = -2uu_x + \varepsilon^2 u_{xx} + \delta u_{xxx}. \quad (2)$$

and

$$u_t + \frac{1}{t}u = -2uu_x + \varepsilon^2 u_{xx} + \delta u_{xxx}. \quad (3)$$

respectively, see [1,2].

The behavior of solutions of the Korteweg–de Vries (KdV) and KdV–Burgers equations was intensively studied for about fifty years. However, these equations remain subjects of various recent studies, mostly in the case of flat waves in one spatial dimension [3–7]. However, cylindrical and spherical waves have a variety of applications (e.g., waves generated by a downhole vibrator), and are studied much less.

We consider the initial value boundary problem (IVBP) for the KdV–Burgers equation on a finite interval:

$$u(x, 0) = f(x), \quad u(a, t) = l(t), \quad u(b, t) = L(t), \quad u_x(b, t) = R(t), \quad x \in [a, b]. \quad (4)$$

In the case $\delta = 0$ (that is, for the Burgers equation), it becomes

$$u(x, 0) = f(x), u(a, t) = l(t), u(b, t) = R(t), x \in [a, b]. \quad (5)$$

The case of the boundary conditions $u(a, t) = A \sin(\omega t)$, $u(b, t) = 0$ and the related asymptotics are of a special interest here. For numerical modeling we use $x \in [0, b]$ instead of \mathbb{R}^+ for appropriately large b .

For the flat wave Burgers equation ($\delta = 0$) the resulting asymptotic profile looks like a periodical chain of shock fronts with a decreasing amplitude (weak breaks or sawtooth waves). If dispersion is non-zero, each wavefront ends with high-frequency micro-oscillations. Further from the oscillator, shock fronts become decaying smooth quasi-periodic oscillations. After the oscillations cease, the wave develops as a constant height and velocity shock. It almost coincides with a traveling wave solution (TWS) of the Burgers equation [8,9].

A traveling wave solution is the solution of the form $u = u(x + Vt)$. Such a solution travels with a constant velocity V along the x -axis, unchanged in its form. The well-known examples are solitons for KdV, shock waves for the Burgers equation. For the existence of TWS for all values of the parameter V it is necessary that an equation has Galilean symmetry.

In the case $\delta = 0$, the Burgers equation has traveling wave solutions, vanishing at $x \rightarrow +\infty$. They are given by the formula [10]

$$u_B(x, t) = \frac{V}{2} \left[1 - \tanh \left(\frac{V}{2\varepsilon^2} (x - Vt + s) \right) \right]; \quad (6)$$

it is used below.

Our aim is to obtain a similar description of a long-time asymptote for cylindrical and spherical waves with periodic boundary conditions. We demonstrate that, in the case of the above IVBP, the perturbation of the equilibrium state for Equations (2) and (3) ultimately takes a form similar to this shock.

This paper is organized as follows. In Section 2, we demonstrate graphs of our numerical experiments for cylindrical/spherical Burgers/KdV–Burgers equations for different combinations to show their the common patterns. In particular we demonstrate that, after the oscillation cease, a solution becomes a monotonic convex line terminated by a head shock.

In Section 3, we find symmetries to Equations (2) and (3). No Galilean symmetry is found, so no real TWS exists. Then equations are brought to a conservation law form, which is later used to obtain rough estimates for the median parameters of the solution. This rough estimate becomes exact for constant boundary conditions, and in Section 4, a very close asymptote for said solution is found in self-similar or homothetic form $u = u(x/t)$.

Yet, at the head shock this asymptotic is unsatisfactory. This head shock moves in unchanged form and with numerically equal velocity and amplitude—exactly as the Burgers traveling wave solution does. In Section 5, using a simple combination of a self-similar approximation and the Burgers traveling wave solution, we obtain the compact closed form approximation. It coincides with a solution in its monotonic part; and this approximation correctly represents the median of the solution in its oscillating part. The quality of the approximation is verified numerically. Connection between the velocity of the solution's head shock and the median value at the start is obtained.

In the section “Conclusions” we formulate main result and discuss the remaining open questions.

2. Typical Examples

Here we demonstrate typical graphs for cylindrical and spherical Burgers waves (see Figures 1 and 2) and for cylindrical and spherical KdV–Burgers (Figures 3 and 4).

We obtained these graphs using the *Maple PDETools package*. The mode of operation used was the default Euler method, which is a centered implicit scheme.

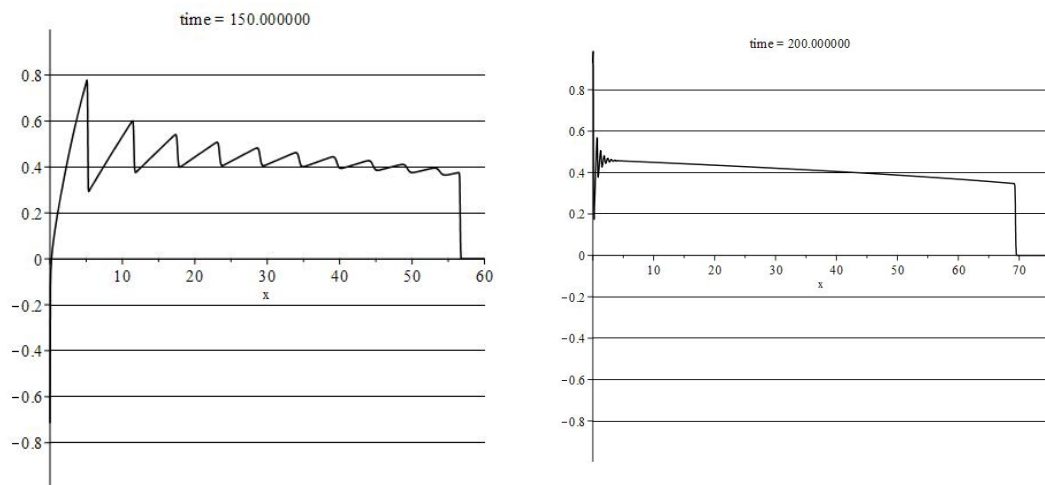


Figure 1. Cylindrical Burgers. $\varepsilon = 0.1$, **Left:** $u_0 = \sin t$, $t = 150$. **Right:** $u_0 = \sin 10t$, $t = 200$.

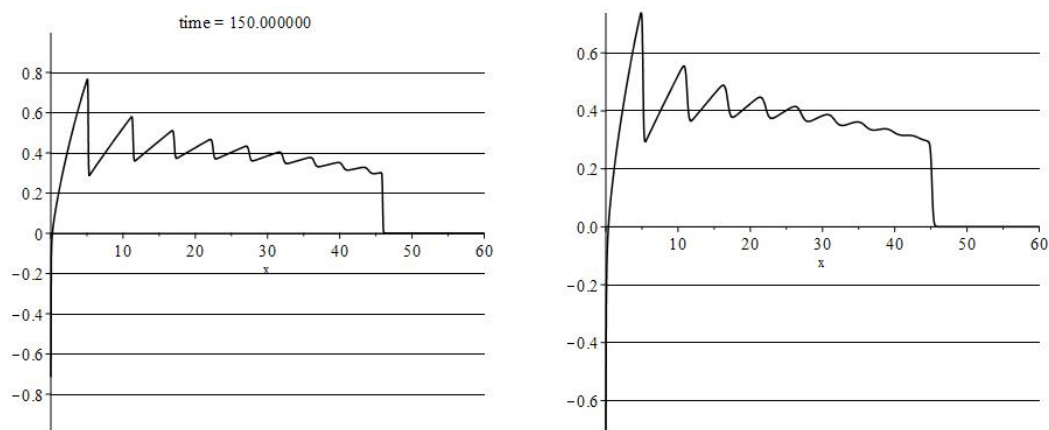


Figure 2. Spherical Burgers, $u_0 = \sin t$. **Left:** $\varepsilon = 0.1$, $t = 150$. **Right:** $\varepsilon^2 = 0.3$, $t = 150$.

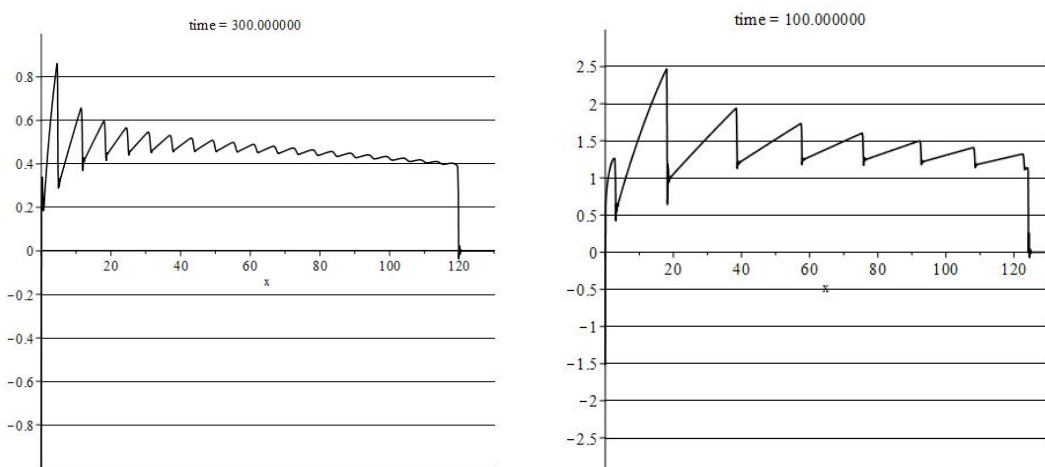


Figure 3. Cylindrical KdV-Burgers. **Left:** $u_0 = \sin t$, $t = 300$, $\varepsilon = 0.1$, $\delta = 0.001$. **Right:** $u_0 = 3 \sin t$, $t = 100$, $\varepsilon = 0.1$, $\delta = 0.001$.

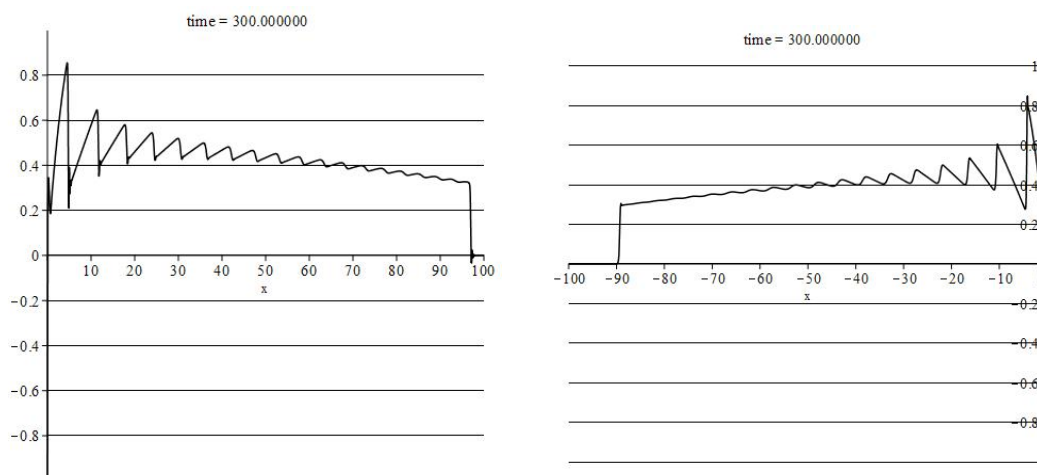


Figure 4. Spherical KdV–Burgers, $u_0 = \sin t$. **Left:** $t = 300, \epsilon = 0.1, \delta = 0.001$. **Right:** $u \leftrightarrow -u, t = 300, \epsilon^2 = 0.02, \delta = 0.001, \epsilon^2 = 0.2$

The solution usually starts with a periodical chain of shock fronts with decreasing amplitudes (sawtooth waves). This weak breaks/sawtooth profile is inherent to periodic waves in dissipative media. Sawtooth waves, their decay, amplitudes, width, etc., were intensively studied in 1970 (see [1,2]) and later. One can also see a common pattern, previously not described, emerging on these figures. After the decay of initial oscillations, graphs become monotonic declining convex lines, terminated by a shock. Recall that for flat waves this monotonic part almost coincides with a constant height traveling wave solution of Burgers equation [7]. The new feature of convex declining lines is caused by the space divergence. We obtain an analytical description of this pattern below.

3. Symmetries and Conservation Laws

3.1. Symmetries

Since cylindrical and spherical equations explicitly depend on time, their stock of symmetries is scarce. For the algorithm of symmetry calculations, see [11]. We found that the algebras of classical symmetries are generated by the following vector fields:

$$X = \frac{\partial}{\partial x}, Y = x \frac{\partial}{\partial x} + 2t \frac{\partial}{\partial t} - u \frac{\partial}{\partial u}, Z = \sqrt{t} \frac{\partial}{\partial x} + \frac{1}{4\sqrt{t}} \frac{\partial}{\partial u}, W = \ln(t) \frac{\partial}{\partial x} + \frac{1}{2t} \frac{\partial}{\partial u}.$$

This list does not contain the Galilean symmetry, so no real traveling wave solution exists.

In particular, symmetry algebra for:

- Cylindrical Burgers is generated by X, Y, Z ;
- Cylindrical KdV–Burgers is generated by X, Z ;
- Spherical Burgers is generated by X, Y, W ;
- Spherical KdV–Burgers is generated by X, W .

3.2. Conservation Laws

First rewrite Equations (1)–(3) into an appropriate conservation law form

$$[t^n \cdot u]_t = [t^n \cdot (-u^2 + \epsilon^2 u_x + \delta u_{xx})]_x, \tag{7}$$

where $n = 0, 1/2, 1$ for flat, cylindrical and spherical cases, respectively.

Hence, for solutions of the above equations we have

$$\oint_{\partial \mathcal{D}} t^n \cdot [u dx + (\epsilon^2 u_x - u^2 + \delta u_{xx}) dt] = 0, \tag{8}$$

where \mathcal{D} is a rectangle

$$\{0 \leq x \leq L, 0 \leq t \leq T\}.$$

While bearing in mind the initial value/boundary conditions $u(x, 0) = u(+\infty, t) = 0$, for $L = +\infty$ the integrals read

$$\int_{+\infty}^0 T^n u(x, T) dx + \int_T^0 t^n (\varepsilon^2 u_x(0, t) - u^2(0, t) + \delta u_{xx}(0, t)) dt = 0.$$

Thus

$$\int_0^{+\infty} u(x, T) dx = \frac{1}{T^n} \int_0^T t^n (-\varepsilon^2 u_x(0, t) + u^2(0, t) - \delta u_{xx}(0, t)) dt. \tag{9}$$

Subsequently

$$\frac{1}{T} \int_0^{+\infty} u(x, T) dx = \frac{1}{T} \int_0^T \frac{1}{T^n} t^n (-\varepsilon^2 u_x(0, t) + u^2(0, t) - \delta u_{xx}(0, t)) dt. \tag{10}$$

The right-hand side of Equation (10) can be computed in some simple cases or estimated. For instance, assume that $\varepsilon^2 u_x(0, t) + \delta u_{xx}(0, t)$ is negligible compared to $u^2(0, t)$. Then

$$\frac{1}{T} \int_0^{+\infty} u(x, T) dx \approx \frac{1}{T} \int_0^T \frac{1}{T^n} t^n (u^2(0, t)) dt = \frac{1}{T} \int_0^T \frac{1}{T^n} t^n (A \sin^2(\omega t)) dt. \tag{11}$$

It follows that

$$n = 0 \Rightarrow \lim_{T \rightarrow \infty} \frac{1}{T} \int_0^T A^2 \sin^2(\omega t) dt = \frac{A^2}{2};$$

$$n = \frac{1}{2} \Rightarrow \lim_{T \rightarrow \infty} \frac{1}{T} \int_0^T \frac{1}{T^{\frac{1}{2}}} t^{\frac{1}{2}} (A \sin^2(\omega t)) dt = \frac{A^2}{3};$$

$$n = 1 \Rightarrow \lim_{T \rightarrow \infty} \frac{1}{T} \int_0^T \frac{1}{T} t (A^2 \sin^2(\omega t)) dt = \frac{A^2}{4}.$$

Another example of exact estimation of right-hand side of Equation (10) is the case of constant boundary conditions.

Consider boundary condition $u(0, t) = M$. The graphs of solution are shown in Figure 5, left (compare their rates of decay caused solely by the spacial dimensions.)

For the resulting compression wave $u_x(0, t) = 0$, the right-hand side of Equation (10) equals

$$\frac{1}{T} \int_0^T \frac{M^2}{T^n} t^n dt = \frac{M^2}{n+1} \tag{12}$$

As the Figures 1–4 show, for a periodic boundary condition, after the decay of initial oscillations, graphs become monotonic convex lines. These convex lines break at $x = V \cdot T$ and at the height V . These monotonic lines are similar to the graphs of constant-boundary solutions; see Figure 5.

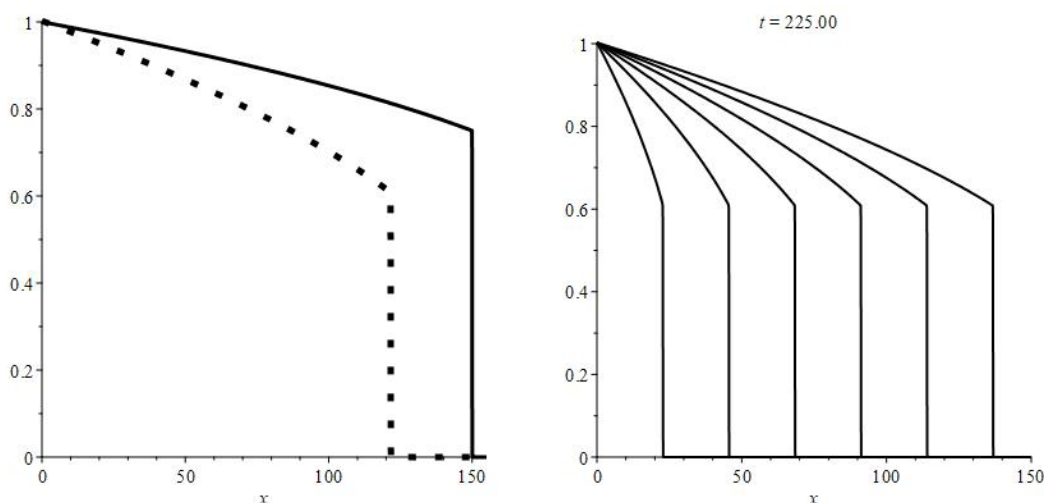


Figure 5. Constant boundary solutions to the Burgers equation, $\varepsilon = 0.1, t = 200$. **Left:** solid line—cylindrical; dotted line—spherical. **Right:** A trace of movement to the right of the spherical solution at moments $t = 37.5 \cdot k, k = 1 \dots 6$.

4. Self-Similar Approximations To Solutions

By observing the solution’s graphs, one can clearly see (e.g., on Figure 5, right) that the monotonic part and its head shock develops as a homothetic transformation of the initial configuration (by t as a homothety parameter). Hence, we seek solutions in the self-similar form, $u(x, t) = y(\frac{x}{t})$. By substituting it into Equations (1)–(3), we get the equation:

$$-y' \frac{x}{t^2} + \frac{ny}{t} = \frac{2yy'}{t} + \frac{\varepsilon^2 y''}{t^2} + \frac{\delta y'''}{t^3}, \tag{13}$$

or

$$-\xi y' + ny = 2yy' + \frac{\varepsilon^2 y''}{t} + \frac{\delta y'''}{t^2}, \tag{14}$$

for $y = y(\xi)$ and $n = 0, 1/2, 1$. For sufficiently large t we may omit last two terms. It follows that appropriate solutions of these truncated ordinary differential equations are given by

$$u_1(x, t) = C_1, C_1 \in \mathbb{R}, n = 0, \text{ for flat waves equation;}$$

$$u_2(x, t) = -\frac{2 + \sqrt{C_2 \xi + 4}}{C_2}, C_2 \in \mathbb{R}, n = \frac{1}{2}, \text{ for cylindrical and}$$

$$u_3(x, t) = \exp\left(\text{LambertW}\left(-\frac{\xi}{2} e^{-\frac{C_3}{2}}\right) + \frac{C_3}{2}\right), C_3 \in \mathbb{R}, n = 1 \text{ for spherical equation.}$$

(The *Lambert W* function, also called the omega function or product logarithm, is a multivalued function, namely, the branches of the inverse relation of the function $f(w) = we^w$, where w is any complex number.

For each integer k there is one branch, denoted by $W_k(z)$, which is a complex-valued function of one complex argument. W_0 is known as the principal branch. When dealing with real numbers the $W_0 = \text{LambertW}$ function satisfies $\text{LambertW}(x) \cdot e^{\text{LambertW}(x)} = x$. The *Lambert W* function, introduced in 1758, has numerous applications in solving equations, mathematical physics, statistics, etc.; for more detail, see [12].)

Let V be the velocity of the signal propagation in the medium. Since at the head shock we have $x = Vt$ and $u = V$, we obtain the condition for finding C_i . It is $y(V) = V$. It follows then that

$$C_1 = V, C_2 = -\frac{3}{V}, C_3 = \ln(V) + \frac{1}{2}.$$

For flat waves, it corresponds to a traveling wave solution of the classical Burgers equation.

For the cylindrical waves, the monotonic part is given by

$$u_2 = \frac{1}{3} \left(2V + V \sqrt{4 - \frac{3x}{Vt}} \right);$$

and for spherical waves

$$u_3 = V \sqrt{e} \exp \left(\text{LambertW} \left(-\frac{x}{2Vt\sqrt{e}} \right) \right).$$

Note that

$$u_2|_{x=0} = \frac{4V}{3} \text{ and } u_3|_{x=0} = V\sqrt{e} \approx 1.65V. \tag{15}$$

These formulas show that the velocity is proportional to the value of a constant boundary solution at $x = 0$.

The corresponding graphs visually coincide with the graphs obtained by numerical modeling; for instance, see a comparison to the solution (at $t = 100$) for the problem

$$u_t = 0.01u_{xx} - 2uu_x - u/t, \quad u(0, t) = 1, u(75, t) = 0, u(x, 0) = 0 \tag{16}$$

in Figure 6, left.

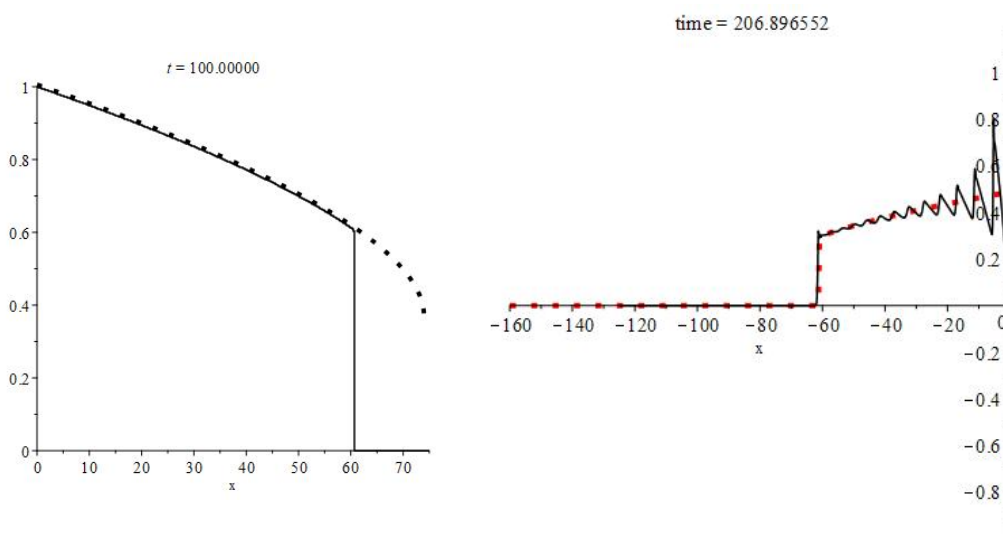


Figure 6. Left: solid line—solution to Equation (16); dotted line—its u_3 approximation. Right: solid line—solution to spherical KdV, $x \rightarrow -x$, $\varepsilon^2 = 0.02$, $\delta = 0.002$; dotted line—its \tilde{u}_3 approximation; both at $t = 200$.

5. Median Approximation

Yet, the monotonic part of the periodic boundary solution ends with a breaking, which travels with a constant velocity and amplitude, very much like the head of the Burgers’ traveling wave solution (Equation (6)). A rather natural idea is to truncate a self-similar solution, multiplying it by a (normalized) formula for the Burgers TWS. Namely, put

- For the cylindrical waves take

$$\tilde{u}_2 = \frac{1}{2} \left[1 - \tanh \left(\frac{V}{\varepsilon^2} (x - Vt) \right) \right] \cdot \frac{1}{3} \left(2V + V \sqrt{4 - \frac{3x}{Vt}} \right); \tag{17}$$

- For spherical waves,

$$\tilde{u}_3 = \frac{1}{2} \left[1 - \tanh\left(\frac{V}{\varepsilon^2}(x - Vt)\right) \right] \cdot V\sqrt{e} \exp\left(\text{LambertW}\left(-\frac{x}{2Vt\sqrt{e}}\right)\right). \quad (18)$$

This construction produces an approximation of astonishing accuracy (see Figure 6, right and Figure 7); these graphs correspond to the spherical KdV–Burgers problem (it comes from Equation) (3) after the change $x \rightarrow -x$.

$$u_t = 0.02u_{xx} + 2uu_x - u/t - 0.002u_{xxx}, \quad u(0, t) = \sin t, u(10, t) = 0, u(x, 0) = 0. \quad (19)$$

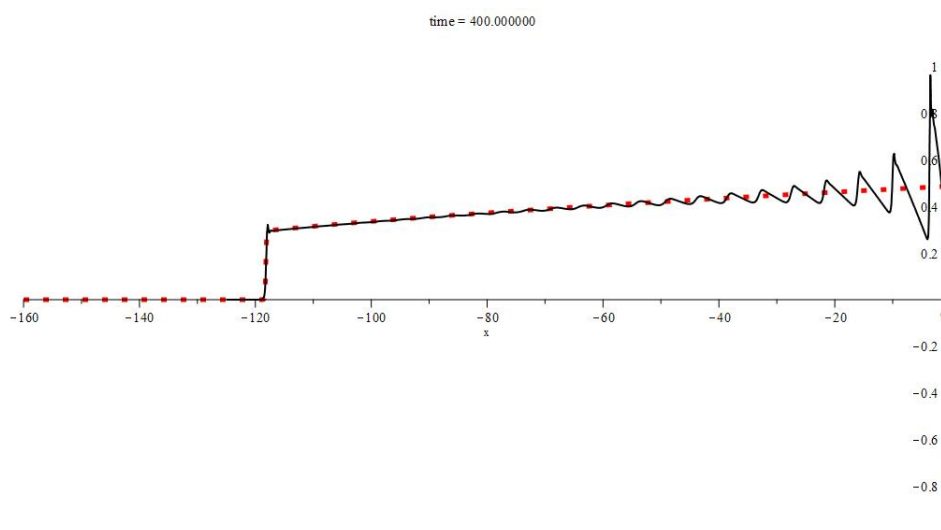


Figure 7. Solid line—solution to spherical KdV, $x \rightarrow -x$, $\varepsilon^2 = 0.02$, $\delta = 0.002$, dotted line—its \tilde{u}_3 approximation; both at $t = 400$.

Moreover, it is evident that the graphs of \tilde{u}_2, \tilde{u}_3 neatly represent the median lines of the approximated solutions over their whole ranges. By median we mean

$$M(x) = (2\pi n/\omega)^{-1} \int_0^{2\pi n/\omega} u(x, t) dt, \quad n \in \mathbb{N}, n \gg 1 (u(0, t) = \sin \omega t).$$

Let us assess the quality of \tilde{u}_2, \tilde{u}_3 approximations numerically. Evaluate the trapezoid area under \tilde{u}_2, \tilde{u}_3 graphs:

- For the cylindrical equation

$$\int_0^{Vt} \left[\frac{1 - \tanh\left(\frac{V}{\varepsilon^2}(x - Vt)\right)}{2} \frac{1}{3} \left(2V + V\sqrt{4 - \frac{3x}{Vt}} \right) \right] dx = \frac{32}{27} V^2 t;$$

- For the spherical equation

$$\int_0^{Vt} \left[\frac{1 - \tanh\left(\frac{V}{\varepsilon^2}(x - Vt)\right)}{2} V\sqrt{e} \exp\left(\text{LambertW}\left(\frac{-x}{2Vt\sqrt{e}}\right)\right) \right] dx = \frac{V^2 t \cdot e}{2}.$$

Hence, the mean value of the left-hand side of (10) can be estimated as follows.

$$\frac{1}{T} \int_0^{+\infty} u(x, T) dx = \frac{1}{T} \int_0^{VT} u(x, T) dx \approx \begin{cases} \frac{32}{27} V^2 & \text{in cylindrical case;} \\ \frac{V^2 \cdot e}{2} & \text{in spherical case,} \end{cases} \quad (20)$$

This mean value can be also evaluated numerically. In the case illustrated by Figure 1 the direct numerical evaluation of the integral differs from the estimation (20) by 1%. It confirms the quality of the approximation.

For constant-boundary waves, it follows from Equation (12) that

$$\frac{M^2}{n+1} = \begin{cases} \frac{32}{27}V^2 & \text{in cylindrical case;} \\ \frac{V^2 \cdot e}{2} & \text{in spherical case;} \end{cases} \quad (21)$$

see Equation (12); of course this result coincides with Equation (15). Hence, the mean value M of an arbitrary solution at the start of oscillations (or in a vicinity of the oscillator) is linearly linked to the velocity of the head shock.

However, to find this mean value for an arbitrary border condition is a tricky task, because the integrands u_x and u_{xx} of the right-hand side of Equation (10) have numerous breaks. Still, one may get an (admittedly rough) estimation for M using Equations (11) and (21). It follows that

$$\frac{M^2}{n+1} \approx \frac{A^2}{k}, \quad k = 2, 3, 4 \quad (22)$$

for flat, cylindrical and spherical cases. In all these cases it results in $M \approx A \frac{\sqrt{2}}{2} \approx 0.71A$.

Numerical experiments also show (e.g., see Figure 3) that for the $u|_{x=0} = A \sin(t)$ boundary condition such a value is $M \approx A \cdot a$, where $a \approx 0.467$ is the mean value for $1 \cdot \sin(t)$ condition. That is, M depends on A almost linearly.

Note that this value may be obtained via the velocity V of the head shock, which, in turn, can be measured with great accuracy by the distance passed by the head shock after a sufficiently long time.

6. Conclusions

In this paper, we studied the pattern formation in periodic boundary solutions of spherical and cylindrical KdV–Burgers equations. Such a solution usually starts with a periodical chain of shock fronts with a decreasing amplitude. When oscillations decay and cease, a solution proceeds as a monotonic convex line that ends with a head shock. This last pattern was not described previously and it is the main subject of the paper.

We obtained simple explicit formulas describing the monotonic part of the solution and its head break. These approximate formulas have great accuracy. Moreover, their graphs neatly represent the median lines of the approximated solutions on their entire ranges. (By median line we mean the level around which the periodical oscillations occur).

To obtain these approximations we used self-similar solutions of the dissipationless and dispersionless KdV–Burgers equation and a traveling wave solution of the flat Burgers equation. Formulas depend on only one parameter: either on the velocity of the signal propagation or on the median value of the solution in the vicinity of the periodic boundary.

Some open questions remain. Our approximations are very good for the one-parameter class of constant boundary solutions. The existence of a one-parameter family of solutions points to the existence of a suitable symmetry, but the classical symmetry analysis was, so far, unhelpful. Conservation laws allows us to assess the value of the approximation's parameter using the boundary condition, but the resulting estimation is rough.

Funding: This work was partially supported by the Russian Basic Research Foundation grant 18-29-10013.

Conflicts of Interest: The author declares no conflict of interest.

Abbreviations

The following abbreviations are used in this manuscript:

KdV	Korteweg–de Vries
IVBP	Initial value boundary problem
TWS	Traveling wave solution

References

1. Leibovich, S.; Seebass, R. (Eds.) *Nonlinear Waves*; Cornell University Press: London, UK, 1974; Chapter 4.
2. Sachdev P.L.; Seebass, R. Propagation of spherical and cylindrical N-waves. *J. Fluid. Mech.* **1973**, *58*, 1973. [[CrossRef](#)]
3. Grava, T. Whitham modulation equations and application to small dispersion asymptotics and long time asymptotics of nonlinear dispersive equations. *arXiv* **2016**, arXiv:1701.00069v1.
4. Chugainova A.P.; Shargatov, V.A. Traveling waves and undercompressive shocks in solutions of the generalized Korteweg–de Vries–Burgers equation with a time-dependent dissipation coefficient distribution. *Eur. Phys. J. Plus* **2020**, *135*, 635. [[CrossRef](#)]
5. Bendaasa, S.; Alaa, N. Periodic Wave Shock Solutions of Burgers Equations, A New Approach. *Int. J. Nonlinear Anal. Appl.* **2020**, *10*, 119–129.
6. Chugainova, A.P.; Shargatov, V.A. Stability of the breaks structure described by the generalized Korteweg-de Vries-Burgers equation. *Comp. Math. Math. Phys.* **2016**, *56*, 259–274 [[CrossRef](#)]
7. Samokhin, A. Periodic boundary conditions for KdV-Burgers equation on an interval. *J. Geom. Physics* **2017**, *113*, 250–256. [[CrossRef](#)]
8. Samokhin, A. Nonlinear waves in layered media: solutions of the KdV—Burgers equation. *J. Geom. Physics* **2018**, *130*, 33–39. [[CrossRef](#)]
9. Samokhin, A. On nonlinear superposition of the KdV-Burgers shock waves and the behavior of solitons in a layered medium. *J. Diff. Geom. Its Appl.* **2017**, *54*, 91–99. [[CrossRef](#)]
10. Whitham, G.B. *Linear and Nonlinear Waves*; John Wiley & Sons: Hoboken, NJ, USA, 1999; ISBN 9781118032954. [[CrossRef](#)]
11. Krasil'shchik I.S.; Vinogradov, A.M. (Eds.) *Symmetries and Conservation Laws for Differential Equations of Mathematical Physics*; American Mathematical Society: Providence RI, USA, 1999; ISSN 0065-9282.
12. Bronstein, M.; Corless, R.M.; Davenport, J.H.; Jeffrey, D.J. Algebraic properties of the Lambert W function from a result of Rosenlicht and of Liouville. In *Integral Transforms and Special Functions*; Taylor & Francis: Abingdon, UK; Volume 19, pp. 709–712. [[CrossRef](#)]